Desalination and Water Treatment
www.deswater.com
doi: 10.5004/dwt.2021.27475

231 (2021) 389–397
August

Batch biosorption of the dye methylene blue from its aqueous solutions by Palm spathe: kinetic, isotherm, and thermodynamic studies

Chawki Djelloul[a], Oualid Hamdaoui[b,*], Abdulaziz Alghyamah[b]

[a]*Laboratory of Reaction Engineering, Faculty of Mechanical Engineering and Process Engineering, USTHB, Algiers, Algeria, email: djelloulchawki@yahoo.fr*
[b]*Chemical Engineering Department, College of Engineering, King Saud University, P.O. Box: 800, 11421 Riyadh, Saudi Arabia, emails: ohamdaoui@ksu.edu.sa (O. Hamdaoui), aalghyamah@ksu.edu.sa (A. Alghyamah)*

Received 20 April 2021; Accepted 30 May 2021

ABSTRACT

The potential of palm spathe (PS), an agricultural waste, to remove methylene blue (MB) from aqueous solution was evaluated in a batch process. The effects of contact time (0–300 min), initial dye concentration (25–400 mg L^{-1}), pH (2–12), temperature (25°C–45°C), ionic strength (0–500 mg L^{-1}) and biosorbent dosage (0.5–6 g L^{-1}) on the uptake of MB by PS were studied. The obtained results show that the optimum pH for MB biosorption was in the range of 5.0–10.0. Increasing the biosorbent concentration from 0.5 to 6 g L^{-1} caused a diminution in biosorption capacity from 59.86 to 8.01 mg g^{-1}. Equilibrium time increased from 120 to 270 min when the initial dye concentration increased from 25 to 400 mg L^{-1}. When the MB concentration augmented from 25 to 400 mg L^{-1}, the amount of MB sorbed increased from 7.83 to 62.62 mg g^{-1}. A rise in temperature from 25°C to 45°C decreased the sorption capacity from 45.28 to 42.36 mg g^{-1}. The removal kinetics was analyzed using the pseudo-first-order and pseudo-second-order model equations. The pseudo-second-order model was found to describe the biosorption process better than the pseudo-first-order equation. Biosorption isotherms were modeled with the Langmuir, Freundlich, and Temkin isotherms. The data fitted well with the Langmuir isotherm. The maximum monolayer biosorption capacity was found to be 74.3 mg g^{-1} at 25°C. The thermodynamic parameters obtained for the sorption of MB by PS demonstrate spontaneous, exothermic, and favorable sorption process. Palm spathe may be used as an alternative biosorbent to remove MB from aqueous solutions.

Keywords: Biosorption; Palm spathe; Methylene blue; Kinetics; Isotherm; Thermodynamic parameters

1. Introduction

Textile dyes and other industrial dyestuffs constitute one of the largest groups of organic compounds that represent an increasing environmental danger [1]. About 1%–20% of the total world production of dyes is lost during the dyeing process and is released in textile effluents [2]. So far, there are more than 100,000 types of dyes, with over 700,000 tons of dyestuff produced annually, which can be classified according to their structure as anionic and cationic [3]. Color interferes with penetration of sunlight into waters, retards photosynthesis, inhibits the growth of aquatic biota, and interferes with gas solubility in water bodies [4]. In addition, dyes can cause severe damage to organism such as dysfunction of kidney, reproductive system, liver, brain, and central nervous system [5]. Methylene blue (MB) is a cationic dye having various applications in chemistry, biology, medical science, and dyeing industries. MB can cause eye burns, and if swallowed, it causes irritation to the gastrointestinal tract with

* Corresponding author.

symptoms of nausea, vomiting, and diarrhea. It may also cause methemoglobinemia, cyanosis, convulsions, and dyspnea if inhaled [6]. Its long-term exposure can cause vomiting, nausea, anemia, and hypertension [7]. Artificial dyes have been in the controversy for many years and scrutinized for being possibly linked to cancer, allergies, and hyperactivity [8].

Various conventional methods of color removal from wastewater have been used. These include biological and physical-chemical processes. Among these techniques, adsorption is a greatly preferred method due to its high efficiency, simplicity in design, and sludge free operation. Activated carbon is the most widely used adsorbent in the adsorption process but it is expensive. There is a need to explore the adsorption potential of the low-cost materials. A number of studies had focused on biomaterials and bio-composites that are capable of removing various pollutants from wastewater [9–39].

One of agriculture wastes that received attention in the present study is the palm spathe (PS). The inflorescence in its early stages is enclosed in a hard covering/envelope known as spathe which splits open as the flowers mature exposing the entire inflorescence for pollination purposes. The average annual number of spathes born by a palm is a dozen for females and more for males. The number of palm trees of different species is estimated at 20 million in Algeria. It is abundant, readily available as a low-cost and environment friendly material.

To the best of our knowledge, the use of raw PS for the biosorption of pollutants from aqueous solutions is until now not examined previously. In this work, we have explored for the first time the potential application of PS as an original biosorbent for the removal of MB from aqueous phase. This issue has been treated for various experimental conditions including contact time (0–300 min), initial dye concentration (25–400 mg L^{-1}), pH (2–12), temperature (25°C–45°C), ionic strength (0–500 mg L^{-1}) and biosorbent dosage (0.5–6 g L^{-1}). Equilibrium isotherm and kinetic data are analyzed and modeled using different equations. Additionally, thermodynamic parameters such as $\Delta G°$, $\Delta S°$, and $\Delta H°$ were determined.

2. Materials and methods

2.1. Biomass and dye solution preparation

After harvesting, the spathes were extracted and cut into pieces and washed with distilled water several times to remove dirt particles and water-soluble materials till the wash water became almost colorless. Then it was oven-dried at 50°C for 3 d and stored in a desiccator until experimental use.

The cationic dye used in this study, methylene blue (MB), was purchased from Sigma-Aldrich (analytical grade). MB chemical formula is $C_{16}H_{18}N_3SCl$. The dye stock solution was prepared by dissolving accurately weighed dye in distilled water to the concentration of 1,000 mg L^{-1}. Distilled water was used for preparing all needed initial concentrations. The dye concentrations were measured by a double beam UV/Vis spectrophotometer (Shimadzu, Model UV 1601, Japan) at 664 nm.

The solution pH was adjusted by the addition of dilute aqueous solutions of HCl or NaOH. Ionic strength of aqueous solutions was adjusted with K_2SO_4 solutions. All reagents used were of analytical grade.

2.2. Batch bisorption experiments

The experiments were carried out in batch mode; all the batch experiments were conducted with 200 mL solutions and stirring speed of 300 rpm. The parameters studied include contact time (0–300 min), initial dye concentration (25–400 mg L^{-1}), pH (2–12), temperature (25°C–45°C), ionic strength (0–500 mg L^{-1}) and biosorbent dosage (0.5–6 g L^{-1}). Samples are taken at different time intervals to monitor the removal of the dye by sorption until equilibrium.

3. Results and discussion

3.1. Influence of pH

The effect of pH on the removal of MB from aqueous solutions by PS was observed at varying pH from 2 to 12 with 25°C temperature, 3 g L^{-1} biosorbent concentration, 50 mg L^{-1} initial dye concentration, and 300 rpm stirring speed.

From Fig. 1, it was observed that the values of the higher sorption capacity at equilibrium (q_e) were recorded at basic pH values, this is maybe due to a significantly high-electrostatic attraction that exists between the negatively charged surface of the biosorbent and cationic dye. Also, the lower sorption capacity at equilibrium was observed at very acidic pH values (2 and 3), this is maybe due to the concurrency between hydronium ions and the cations of the MB. Also, the surface of the biosorbent was protonated with excessive H^+, making the sites of the biosorbent positively charged with strong electrostatic repulsion for cations [40,13]. On the other hand, the sorption capacities for the other pH values have not much significant difference. The values of the sorption capacities at equilibrium are between 15 and 16 mg g^{-1} for pH varying between 4 and 12, while they are 7 and 12 mg g^{-1} for pH 2 and 3, respectively. This is why the next experiments will be carried out at natural pH (5.3).

3.2. Influence of biosorbent concentration

The effect of biosorbent concentration on the sorption capacity and percentage of removal of MB was investigated using 200 mL of aqueous solution with initial dye concentration (C_0) of 50 mg L^{-1} with 25°C temperature, natural pH (5.3), and 300 rpm stirring speed. The biosorbent amount was varied from 0.1 to 1.2 g. It is observed from Fig. 2 that the increase in the concentration of biosorbent led to an increase in the percentage of removal from 59.86% to 96.08%, this is because of the larger number of active sites available for the biosorption provided by a larger amount of biosorbent mass. However, increasing the biosorbent concentration from 0.5 to 6 g L^{-1} caused a decrease in biosorption capacity from 59.86 to 8.01 mg g^{-1}. This is because, for a fixed initial dye concentration, the amount of dye was shared over a larger mass as the dose of the

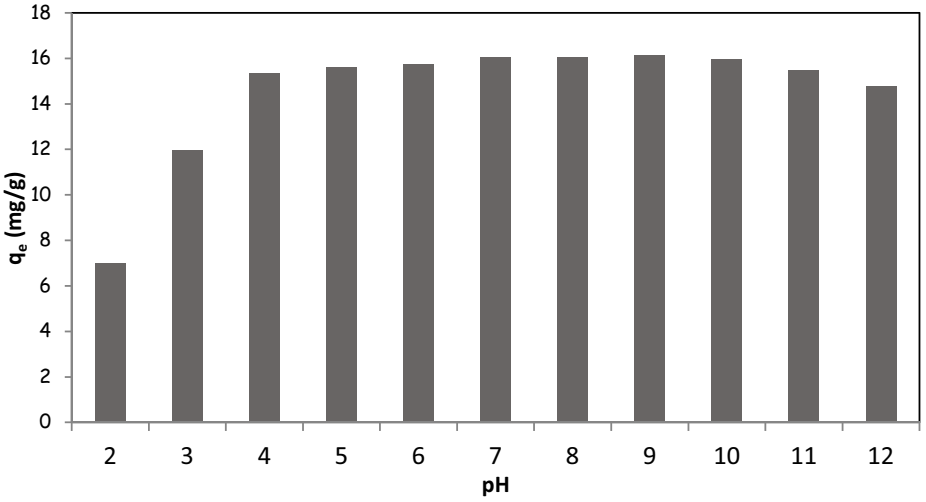

Fig. 1. Effect of pH on the biosorption capacity of methylene blue (sorbent concentration = 3 g L^{-1}, dye concentration = 50 mg L^{-1}, temperature = 25°C).

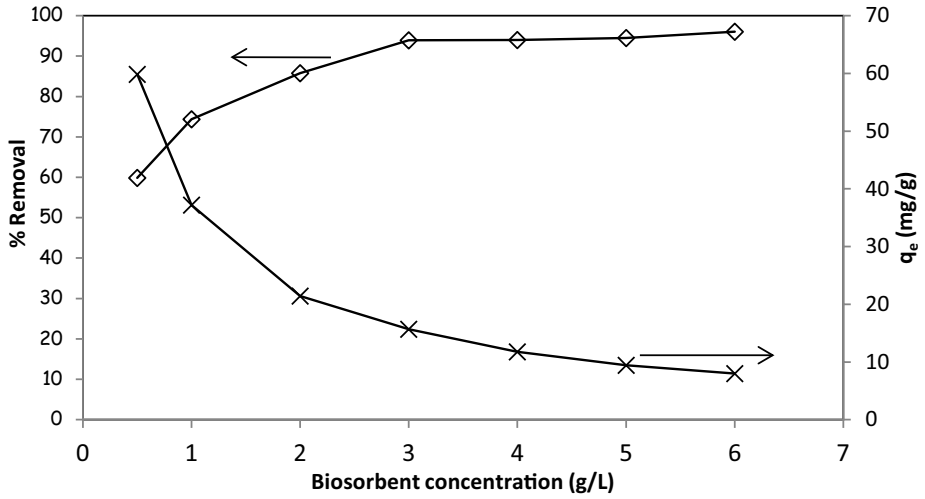

Fig. 2. Effect of sorbent concentration on the biosorption capacity and removal percentage of MB (dye concentration = 50 mg L^{-1}, temperature = 25°C, pH = 5.3).

sorbent increased, therefore, the dye sorbed per unit of biosorbent mass decreased. Similar results were reported for dye sorption [41]. The increase in the percentage of removal is no longer significant when the sorbent concentration exceeds 3 g L^{-1}.

3.3. Influence of initial dye concentration and contact time

The biosorption of the dye was studied as a function of contact time, for different initial concentrations, in order to determine the required time for maximum sorption. The results are shown in Fig. 3. The biosorption at all dye concentrations rapidly increased initially and then gradually augmented until equilibrium was attained. It was observed that as the initial MB concentration increases, the equilibrium time increases. Equilibrium time increases from 120 to 270 min when the initial dye concentration increases from 25 to 400 mg L^{-1}. The decreased biosorption rate, particularly, toward the end of experiments, indicates the possible monolayer formation of MB on the biosorbent surface [42,43]. Also, the sorption capacity was observed to increase with an increasing of initial concentration of dye. When the MB concentration increased from 25 to 400 mg L^{-1}, the amount of MB sorbed increased from 7.83 to 62.62 mg g^{-1}. The increase of initial dye concentration provided an increase in the biosorption capacity, since higher concentrations contribute to a decrease in mass transfer resistance of solution to the sorbent surface, thus filling possible active sites still unoccupied at low dye concentrations [44,45].

3.4. Influence of ionic strength

The influence of ionic strength on the sorption of MB by PS was studied with a constant initial dye concentration

of 50 mg L^{-1}, a sorbent concentration of 3 g L^{-1}, a natural pH, and a temperature of 25°C. The ionic strength of the dye solution was modified using different dosages of K_2SO_4 (0–500 mg L^{-1}). The ionic strength disfavors the sorption of dye (figure not shown), the biosorption capacity decreases slightly as K_2SO_4 concentration increases, when the salt concentration increased from 0 to 500 mg L^{-1}, the amount of sorbed MB decreased from 15.66 to 13.59 mg g^{-1}. This is because K^+ ions in the aqueous phase compete effectively with positively charged dye cation for the same binding sites on the biosorbent surface. Additionally, salt screens the electrostatic interaction between sorbent and sorbate [46]. A similar trend was reported for the sorption of MB by milk thistle seeds [47]. This result is different from those reported by Dogan et al. [48]; where the dye adsorption slightly increases with the increasing salt (NaCl) concentration, and it is also different from those reported by Janos et al. [49]; they tested the effect of inorganic salts (NaCl and $CaCl_2$) on some acid and basic dye adsorption and found that the dye adsorption was not affected.

3.5. Influence of temperature

The effect of temperature was investigated from batch experiments carried out at three constant temperatures 25°C, 35°C and 45°C with a constant initial dye concentration of 50 mg L^{-1}, a sorbent concentration of 3 g L^{-1}, and natural pH. An increase in temperature from 25°C to 45°C decreased the percentage removal from 90.55% to 84.73% (figure not shown), which corresponds to a decrease of sorption capacity from 45.28 to 42.36 mg g^{-1}, respectively, indicating the exothermic nature of the biosorption process. This can be explained by the exothermicity of the sorption process and by the weakening of the bonds between the dye and the active sites of the sorbent for the highest temperatures. The high sorption rate at the beginning of sorption at high temperatures was due to the rate of diffusion of the dye molecules across the external boundary layer, due to the decrease in the viscosity of the solution. Similar temperature effect was reported for MB dye sorption onto melon peel [50] and milk thistle seeds [47].

3.6. Biosorption kinetics modeling

Biosorption kinetics is one of the most important parameters in process design, which is important due to controlling the process efficiency, describing the sorption rate, and determining the optimal practical conditions [51].

The modeling of the effect of initial dye concentration using the pseudo-first-order and pseudo-second-order kinetics proposed by Lagergren [52] and Blanchard [53,54], respectively, was applied to understand the sorption kinetics.

The linear forms of the pseudo-first and pseudo-second-order equations are given, respectively, as follows:

$$\ln\left(q_e - q\right) = \ln q_e - k_1 t \tag{1}$$

$$\frac{t}{q} = \frac{1}{k_2 q_e^2} + \frac{1}{q_e} t \tag{2}$$

where q_e and q are the amounts of MB sorbed (mg g^{-1}) at equilibrium and at time t (min), respectively, k_1 is the rate constant of pseudo-first-order sorption (min^{-1}) and k_2 is the rate constant of pseudo-second-order sorption (g mg^{-1} min^{-1}). The initial sorption rate, h (mg g^{-1} min^{-1}) is expressed as:

$$h = k_2 q^2 \tag{3}$$

Plotting $\ln(q_e - q)$ versus time for the various initial dye concentrations (figure not shown) allows for the calculations of pseudo-first-order parameters, k_1 and q_e. Similarly, the pseudo-second-order kinetic constant, k_2 (g mg^{-1} min^{-1}), the initial sorption rate and the amount of dye sorbed at equilibrium, q_e (mg g^{-1}), can be calculated from the intercept and slope of the plot between t/q vs. t (Fig. 4). Kinetic parameters and the corresponding r^2 values are shown in Table 1. From Table 1, the low r^2 values and the q_e values predicted using the Lagergren plot fails to predict the q_e values for all initial dye concentrations studied. Unlike Blanchard's model, the relatively higher r^2 value (>0.99) for pseudo-second-order kinetics and the convergence between the theoretically predicted q_e and the experimental

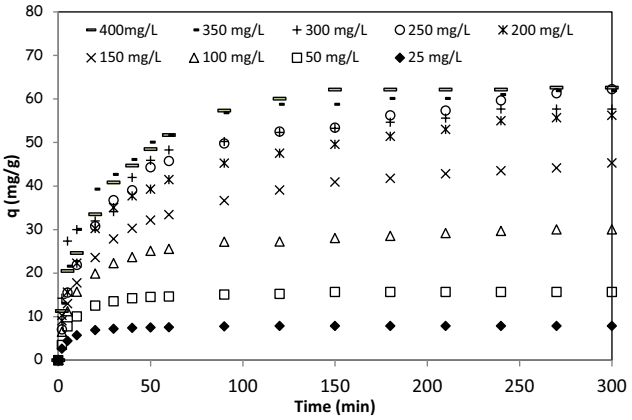

Fig. 3. Effect of contact time and initial concentration of the dye on the sorption of MB by PS (temperature = 25°C, sorbent concentration = 0.6 g/0.2 L solution, stirring speed = 300 rpm, pH = 5.3).

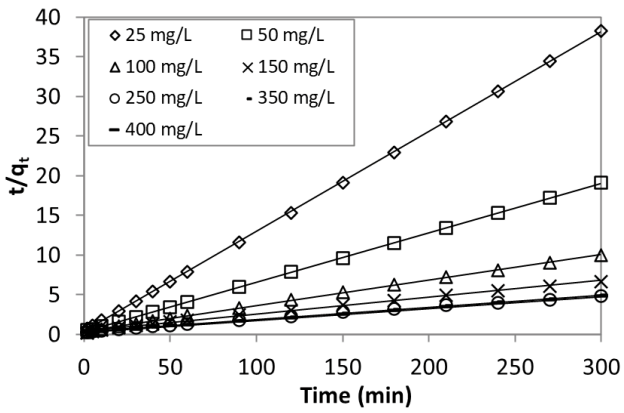

Fig. 4. Modeling of MB sorption kinetics by PS at various initial dye concentrations using the pseudo-second-order model.

Table 1
Pseudo-first-order and pseudo-second-order kinetic models constants and determination coefficients at various initial dye concentrations

		Pseudo-first-order model			Pseudo-second-order model			
C_0 (mg L^{-1})	q_e(exp) (mg g^{-1})	r^2	k_1 (min^{-1})	q_e (cal) (mg g^{-1})	r^2	k_2 (g mg^{-1} min^{-1})	q_e (cal) (mg g^{-1})	h (mg g^{-1} min^{-1})
25	7.83	0.9364	0.0431	3.3059	0.99995	0.04022	7.94281	2.54
50	15.66	0.8758	0.0267	6.6006	0.99991	0.01114	16.02307	2.86
100	30.01	0.9426	0.0146	14.5554	0.99935	0.00285	30.88326	2.72
150	45.28	0.9855	0.0119	27.8087	0.99745	0.00110	46.99248	2.43
200	56.25	0.9611	0.0137	38.9937	0.99690	0.00082	58.82353	2.84
250	62.25	0.9521	0.0122	42.8626	0.99700	0.00065	65.23157	2.78
300	57.68	0.9549	0.0135	30.4809	0.99780	0.00115	60.02401	4.15
350	61.91	0.9528	0.0156	31.9190	0.99954	0.00124	64.26735	5.12
400	62.62	0.9746	0.0288	55.1689	0.99892	0.00098	66.44518	4.31

q_e values, suggested that the sorption of MB by PS follows a pseudo-second-order kinetics. This confirmed that the rate-limiting step is chemisorption, involving valence forces through sharing or exchange of electrons [6,55].

3.7. Biosorption isotherm modeling

The equilibrium isotherms in this study were analyzed using the Langmuir, Freundlich, and Temkin isotherms. The Langmuir isotherm theory assumes monolayer coverage of sorbate over a homogenous sorbent surface [56]. Freundlich isotherm is an experimental model based on sorption on heterogeneous surfaces [57]. Temkin and Pyzhev [58] considered the effects of some indirect sorbate/sorbate interactions on sorption isotherms and suggested that because of these interactions the heat of sorption of all the molecules in the layer would decrease linearly with coverage. The Langmuir, Freundlich, and Temkin isotherms are given by the following equations, respectively:

$$\frac{C_e}{q_e} = \frac{1}{bq_m} + \frac{1}{q_m}\frac{1}{C_e} \tag{4}$$

where q_e (mg g^{-1}) and C_e (mg L^{-1}) are the equilibrium sorption capacity and equilibrium dye concentration, respectively, q_m (mg g^{-1}) is the maximum sorption capacity and b (L mg^{-1}) is the Langmuir constant related to the free energy of sorption.

$$\ln q_e = \ln K_F + \frac{1}{n}\ln C_e \tag{5}$$

where n and K_F ($mg^{1-1/n}$ $L^{1/n}$ g^{-1}) are Freundlich constants indicative of the intensity of the sorption and the relative sorption capacity of the sorbent, respectively.

$$\ln q_e = \frac{RT}{b_t}\ln a_t + \frac{RT}{b_t}\ln C_e \tag{6}$$

where b_t is the Temkin constant related to the heat of sorption (J mol^{-1}), a_t is the Temkin isotherm constant (L mg^{-1}), R is the universal gas constant (8.314 J mol^{-1} K^{-1}) and T is the absolute temperature (K).

These three equations were fitted to the experimental equilibrium data for MB at different temperatures and the obtained results are plotted in Figs. 5–7.

In the present study in addition to the widely used, r^2, the average percentage error (APE) is used to minimize the error distribution between the experimental equilibrium data and predicted isotherms. The average percentage errors (APE) are calculated as follows:

$$\text{APE}(\%) = \frac{\sum_{1}^{N}\left|\frac{q_{e_{\text{exp}}} - q_{e_{\text{cal}}}}{q_{e_{\text{exp}}}}\right|}{N} \times 100 \tag{7}$$

The subscripts 'exp' and 'cal' show the experimental and calculated values, respectively, and N is the number of experimental data.

The model's parameter values, the values of APE and determination coefficients are shown in Table 2. According to Freundlich and Temkin sorption isotherms, the fitting r^2 for different temperatures are less than 0.973 and 0.983, respectively. While, the fitting r^2 with Langmuir sorption isotherm for temperatures of 25°C, 35°C, and 45°C are 0.992, 0.994, and 0.990, respectively. Also, the values of APE, using the Langmuir model, for different temperatures are the smallest, showing that the equilibrium experimental data was better described by the Langmuir equation with a maximum sorption capacity q_m of 74.3 mg g^{-1} at 25°C. According to the exothermic nature of the sorption process, the maximum sorption capacity decreases with an increase in temperature. Various treated biosorbents have been applied in the removal of MB from the aqueous solution, as reported in the previous literature, for comparison purposes. These results can be compared with other authors in term of the maximum sorption capacity: activated carbon developed from Ficus Carica bast (q_m = 47.62 mg/g) [6], modified Pumice Stone (q_m = 106.383 mg/g) [59], Carica papaya wood (q_m = 32.25 mg/g) [60], Potato shell (q_m = 48.7 mg/g) [61], *Scenedesmus* (q_m = 61.69 mg/g) [62],

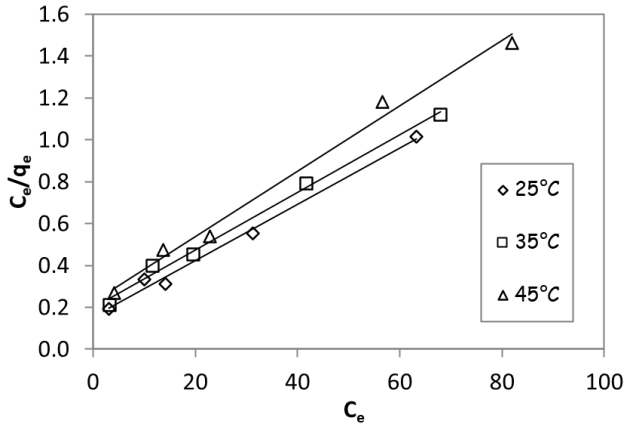

Fig. 5. Langmuir plot for the sorption of MB by PS at different temperatures (conditions: initial dye concentration = 25–400 mg L^{-1}; sorbent dosage = 0.6 g/200 mL; stirring speed = 300 rpm; pH 5.3).

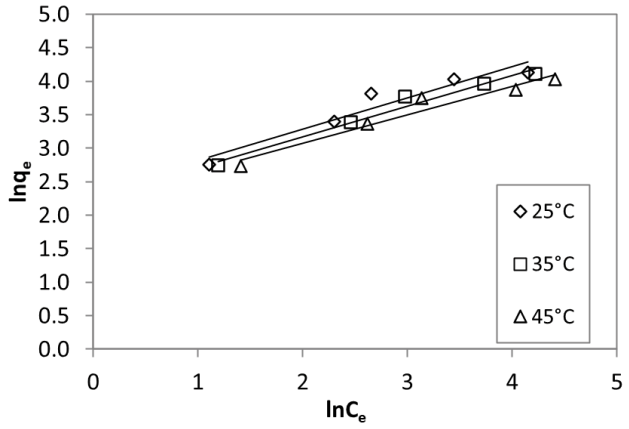

Fig. 6. Freundlich plot for the sorption of MB by PS at different temperatures (conditions: initial dye concentration = 25–400 mg L^{-1}; sorbent dosage = 0.6 g/200 mL; stirring speed = 300 rpm; pH 5.3).

Paspalum maritimum (q_m = 56.18 mg/g) [45]. It is concluded that untreated palm spathe is amongst the most efficient sorbents and has the potential to be used as a biosorbent for the removal of MB from aqueous solutions.

The essential characteristics of the Langmuir isotherm can be expressed in terms of a dimensionless constant separation factor "R_L" that is given by the following equation [63]:

$$R_L = \frac{1}{1 + b \times C_0} \tag{8}$$

where C_0 (mg L^{-1}) is the initial concentration of dye and b (L mg^{-1}) is the Langmuir constant. The values of R_L indicate the type of isotherm to be irreversible (R_L = 0), favorable (0 < R_L < 1), linear (R_L = 1), or unfavorable (R_L > 1). From Fig. 8, the values of R_L in the present investigation have been found less than 1 at 25°C–45°C indicating that the biosorption of MB by PS is favorable. Similar results were reported for dye sorption [6].

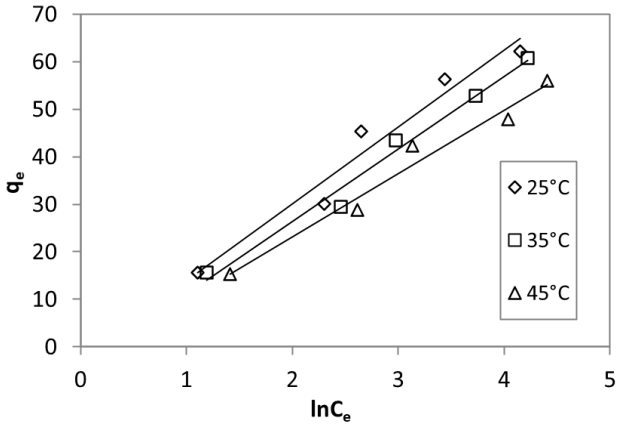

Fig. 7. Temkin plot for the sorption of MB by PS at different temperatures (conditions: initial dye concentration = 25–400 mg L^{-1}; sorbent dosage = 0.6 g/200 mL; stirring speed = 300 rpm; pH 5.3).

Table 2
Isotherm constants for methylene blue biosorption by Palm spathe

	25°C	35°C	45°C
Langmuir			
b (L mg^{-1})	0.0871	0.0699	0.0691
q_m (mg g^{-1})	74.2942	72.6216	64.0205
r^2	0.9919	0.9937	0.9897
APE (%)	9.1	5.1	7.3
Freundlich			
n	2.1306	2.1835	2.3562
K_F ($mg^{1-(1/n)}L^{1/n}g^{-1}$)	10.4239	9.5702	9.2206
r^2	0.9259	0.9726	0.9476
APE (%)	19.9	16.7	18.4
Temkin			
a_t (L mg^{-1})	0.8653	0.7672	0.7645
b_t (J mol^{-1})	152.8907	168.1170	198.0566
r^2	0.9585	0.9825	0.9710
APE (%)	16.8	12.7	12.4

3.8. Thermodynamic parameters of sorption

Thermodynamic parameters evaluated for MB sorption by PS are the free energy change ($\Delta G°$), enthalpy change ($\Delta H°$) and entropy change ($\Delta S°$). It is possible to calculate Gibbs energy changes for the sorption process by using the equilibrium constant (b) obtained for each temperature from the Langmuir model according to the following equation:

$$\Delta G° = -RT\ln b \tag{9}$$

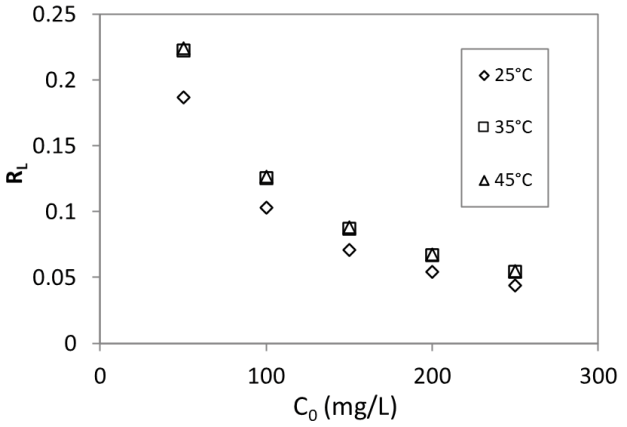

Fig. 8. The separation factor for MB sorption by PS at different temperatures.

where R is the universal gas constant, b is the equilibrium constant, T is the temperature (K) and $\Delta G°$ is the free energy change (J/mol).

The enthalpy and entropy changes of sorption can be determined through the slope and intercept of the line produced by drawing $\Delta G°$ vs. T according to the following equation:

$$\Delta G° = \Delta H° - T\Delta S° \quad (10)$$

The negative values of the standard Gibbs free energy at various temperatures (–25.358 kJ mol^{-1} at 298 K, –25.646 kJ mol^{-1} at 308 K and –26.449 kJ mol^{-1} at 318 K) indicated the spontaneous nature of the sorption of MB by PS. In accord with temperature effect, the negative value of the standard enthalpy (–9.023 kJ mol^{-1}) indicates the exothermic nature of the sorption of MB by the biosorbent. Positive value of the entropy change (51.53 J mol^{-1} k^{-1}) corresponds to an increase in the degree of freedom of the sorbed species.

4. Conclusion

The palm spathe is a locally available, low-cost material and can be used as an alternative sorbent for the removal of MB or other cationic dyes from aqueous solutions without any chemical, heat, or other pretreatment. The biosorption of MB depended on pH and temperature; the optimum pH was in the range of 5.0–10.0, and the sorption is favored by low temperatures. The ionic strength disfavors the sorption of dye.

The removal of MB increases by increasing sorbent dosage. Increasing the initial concentration of MB leads to an increase in sorption.

Kinetic results for the biosorption of MB by PS were better described by the pseudo-second-order model. Equilibrium data fitted very well with Langmuir isotherm equation. The maximum monolayer sorption capacity was found to be 74.3 mg g^{-1} at 25°C. Thermodynamic parameters show that the sorption of MB by PS is spontaneous, favorable, and exothermic.

Therefore, the biosorbent is expected to be successfully utilized as a low-cost, alternative, eco-friendly, and effective sorbent for the removal of MB dye from aqueous solutions.

Acknowledgements

The authors extend their appreciation to the Deanship of Scientific Research at King Saud University for funding this work through research group No. RG-1441-501.

References

[1] S. Bekkouche, S. Merouani, O. Hamdaoui, M. Bouhelassa, Efficient photocatalytic degradation of Safranin O by integrating solar-UV/TiO_2/persulfate treatment: implication of sulfate radical in the oxidation process and effect of various water matrix components, J. Photochem. Photobiol., A, 345 (2017) 80–91.
[2] H. Zollinger, Color Chemistry: Synthesis, Properties and Application of Organic Dyes and Pigments, VCH Publishers, New York, 2004.
[3] Y.S.A. Degs, M.I.E. Barghouthi, A.H.E. Sheikh, G.M. Walker, Effect of solution pH, ionic strength, and temperature on adsorption behavior of reactive dyes on activated carbon, Dyes Pigm., 77 (2008) 16–23.
[4] H. Ghodbane, O. Hamdaoui, S. Merouani, Degradation of C.I. Acid Blue 25 in water using UV/$K_2S_2O_8$ process: effect of salts and environmental matrix, Desal. Water Treat., 74 (2017) 395–401.
[5] N.K. Amin, Removal of direct blue-106 dye from aqueous solution using new activated carbons developed from pomegranate peel: adsorption equilibrium and kinetics, J. Hazard. Mater., 165 (2009) 52–62.
[6] D. Pathania, S. Sharma, P. Singh, Removal of methylene blue by adsorption onto activated carbon developed from *Ficus carica* bast, Arab. J. Chem., 10 (2017) 1445–1451.
[7] S. Senthilkumaar, P.R. Varadarajan, K. Porkodi, C.V. Subbhuraam, Adsorption of methylene blue onto jute fiber carbon: kinetics and equilibrium studies, J. Colloid Interface Sci., 284 (2005) 78–82.
[8] J. Mittal, Permissible synthetic food dyes in India, Resonance – J. Sci. Educ., 25 (2020) 567–577.
[9] Y.A. Argun, A. Karacali, U. Calisir, N. Kilinc, H. Irak, Biosorption method and biosorbents for dye removal from industrial wastewater: a review, Int. J. Adv. Res., 5, (2017) 707–714.
[10] M.S. Alam, R. Khanom, M.A. Rahman, Removal of Congo Red Dye from industrial wastewater by untreated sawdust, Am. J. Environ. Prot., 4 (2015) 207–213.
[11] M.F. Dahr, H. Abolghasemi, M. Esmailia, A. Shojamoradi, H. Fatoorehchi, Adsorption characteristics of Congo Red from aqueous solution onto tea waste, Chem. Eng. Commun., 202 (2015) 181–193.
[12] K.Y. Omidi, R. Heydari, H. Nourmoradi, H. Basiri, H. Basiri, Low-cost sorbent for the removal of aniline and methyl orange from liquid-phase: Aloe Vera leaves wastes, J. Taiwan Inst. Chem. Eng., 68 (2016) 90–98.
[13] M. Gupta, H. Gupta, D.S. Kharat, Adsorption of Cu(II) by low cost adsorbents and the cost analysis, Environ. Technol. Innovation, 10 (2018) 91–101.
[14] Y. Safa, S.R. Tariq, H.N. Bhatti, M. Sultan, I. Bibi, S. Nouren, Synthesis and characterization of sugarcane bagasse/zinc aluminium and apple peel/zinc aluminium biocomposites: application for removal of reactive and acid dyes, Membr. Water Treat., 9 (2018) 301–307.
[15] H.N. Bhatti, Y. Safa, S.M. Yakout, O.H. Shair, M. Iqbal, A. Nazir, Efficient removal of dyes using carboxymethyl cellulose/alginate/polyvinyl alcohol/rice husk composite: adsorption/desorption, kinetics and recycling studies, Int. J. Biol. Macromol., 150 (2020) 861–870.
[16] S. Noreen, H.N. Bhatti, M. Iqbal, F. Hussain, F.M. Sarim, Chitosan, starch, polyaniline and polypyrrole biocomposite

with sugarcane bagasse for the efficient removal of Acid Black dye, Int. J. Biol. Macromol., 147 (2020) 439–452.
[17] M. Maqbool, H.N. Bhatti, S. Sadaf, M. Zahid, M. Shahid, A robust approach towards green synthesis of polyaniline-Scenedesmus biocomposite for wastewater treatment applications, Mater. Res. Express, 6 (2019) 055308.
[18] U. Kamran, H.N. Bhatti, M. Iqbal, S. Jamil, M. Zahid, Biogenic synthesis, characterization and investigation of photocatalytic and antimicrobial activity of manganese nanoparticles synthesized from *Cinnamomum verum* bark extract, J. Mol. Struct., 1179 (2019) 532–539.
[19] I. Anastopoulos, A. Mittal, M. Usman, J. Mittal, G. Yu, A.N. Delgado, M. Kornaros, A review on halloysite-based adsorbents to remove pollutants in water and wastewater, J. Mol. Liq., 269 (2018) 855–868.
[20] C. Arora, S. Soni, S. Sahu, J. Mittal, P. Kumar, P.K. Bajpai, Iron based metal organic framework for efficient removal of methylene blue dye from industrial waste, J. Mol. Liq., 284 (2019) 343–352.
[21] S. Soni, P.K. Bajpai, J. Mittal, C. Arora, Utilisation of cobalt doped iron based MOF for enhanced removal and recovery of methylene blue dye from waste water, J. Mol. Liq., 314 (2020) 113642.
[22] I. Anastopoulos, I. Pashalidis, A.G. Orfanos, I.D. Manariotis, T. Tatarchuk, L. Sellaoui, A.B. Petriciolet, A. Mittal, A.N. Delgado, Removal of caffeine, nicotine and amoxicillin from (waste)waters by various adsorbents. A review, J. Environ. Manage., 261 (2020) 110236.
[23] V. Kumar, P. Saharan, A.K. Sharma, A. Umar, I. Kaushal, A. Mittal, Y.A. Hadeethi, B. Rashad, Silver doped manganese oxide-carbon nanotube nanocomposite for enhanced dye-sequestration: isotherm studies and RSM modelling approach, Ceram. Int., 46 (2020) 10309–10319.
[24] V.K. Gupta, S. Agarwal, R. Ahmad, A. Mirza, J. Mittal, Sequestration of toxic Congo red dye from aqueous solution using ecofriendly guar gum/activated carbon nanocomposite, Int. J. Biol. Macromol., 158 (2020) 1310–1318.
[25] A. Mittal, L. Kurup, Column operations for the removal and recovery of a hazardous dye 'acid red 27' from aqueous solutions, using waste materials – bottom ash and de-oiled soya, Eco. Environ. Conserv., 12 (2006) 181–186.
[26] A. Mittal, R. Ahmad, I. Hasan, Poly (methyl methacrylate)-grafted alginate/Fe_3O_4 nanocomposite: synthesis and its application for the removal of heavy metal ions, Desal. Water Treat., 57 (2016) 19820–19833.
[27] A. Mittal, R. Ahmad, I. Hasan, Biosorption of Pb^{2+}, Ni^{2+} and Cu^{2+} ions from aqueous solutions by L-cystein-modified montmorillonite-immobilized alginate nanocomposite, Desal. Water Treat., 57 (2016) 17790–17807.
[28] A. Mittal, R. Ahmad, I. Hasan, Iron oxide-impregnated dextrin nanocomposite: synthesis and its application for the biosorption of Cr(VI) ions from aqueous solution, Desal. Water Treat., 57 (2016) 15133–15145.
[29] R. Ahmad, I. Hasan, A. Mittal, Adsorption of Cr(VI) and Cd(II) on chitosan grafted polyaniline-OMMT nanocomposite: isotherms, kinetics and thermodynamics studies, Desal. Water Treat., 58 (2017) 144–153.
[30] H. Daraei, A. Mittal, Investigation of adsorption performance of activated carbon prepared from waste tire for the removal of methylene blue dye from wastewater, Desal. Water Treat., 90 (2017) 294–298.
[31] H. Draei, A. Mittal, M. Noorisepehr, F. Daraei, Kinetic and equilibrium studies of adsorptive removal of phenol onto eggshell waste, Environ. Sci. Pollut. Res., 20 (2013) 4603–4611.
[32] A. Mittal, V. Thakur, V. Gajbe, Evaluation of adsorption characteristics of an anionic azo dye Brilliant Yellow onto hen feathers in aqueous solutions, Environ. Sci. Pollut. Res., 19 (2012) 2438–2447.
[33] J. Mittal, V. Thakur, A. Mittal, Batch removal of hazardous azo dye Bismark Brown R using waste material hen feather, Ecol. Eng., 60 (2013) 249–253.
[34] A. Mittal, J. Mittal, Hen Feather, A Remarkable Adsorbent for Dye Removal, Green Chemistry for Dyes Removal from Wastewater, S.K. Sharma, ed., Scrivener Publishing LLC, USA, 2015, pp. 409–457.
[35] O. Hamdaoui, Intensification of the sorption of Rhodamine B from aqueous phase by loquat seeds using ultrasound, Desalination, 271 (2011), 279–286.
[36] E. Guechi, O. Hamdaoui, Biosorption of methylene blue from aqueous solution by potato (Solanum tuberosum) peel: equilibrium modelling, kinetic, and thermodynamic studies, Desal. Water Treat., 57 (2016) 10270–10285.
[37] E. Guechi, O. Hamdaoui, Evaluation of potato peel as a novel adsorbent for the removal of Cu(II) from aqueous solutions: equilibrium, kinetic, and thermodynamic studies, Desal. Water Treat., 57 (2016) 10677–10688.
[38] M. Zamouche, O. Hamdaoui, Sorption of Rhodamine B by cedar cone: effect of pH and ionic strength, Energy Procedia, 18 (2012) 1228–1239.
[39] C. Djelloul, O. Hamdaoui, Dynamic adsorption of methylene blue by melon peel in fixed-bed columns, Desal. Water Treat., 56 (2015) 2966–2975.
[40] E. Sharifpour, H.Z. Khafri, M. Ghaedi, A. Asfaram, R. Jannesar, Isotherms and kinetic study of ultrasound-assisted adsorption of malachite green and Pb^{2+} ions from aqueous samples by copper sulfide nanorods loaded on activated carbon: experimental design optimization, Ultrason. Sonochem., 40 (2018) 373–382.
[41] E. Aladağ, B.A. Fil, R. Boncukcuoğlu, O. Sözüdoğru, A.E. Yılmaz, Adsorption of methyl violet dye, a textile industry effluent onto montmorillonite—batch study, J. Dispersion Sci. Technol., 35 (2014) 1737–1744.
[42] M.M.A.E. Latif, A.M. Ibrahim, Adsorption, kinetic and equilibrium studies on removal of basic dye from aqueous solutions using hydrolyzed oak sawdust, Desal. Water Treat., 6 (2009) 252–268.
[43] A.E. Nemr, W.O. Abdel, E.S. Amany, A. Khaled, Removal of direct blue-86 from aqueous solution by new activated carbon developed from orange peel, J. Hazard. Mater, 161 (2009) 102–110.
[44] S.M. Miraboutalebi, S.K. Nikouzad, M. Peydayesh, N. Allahgholi, L. Vafajoo, G. McKay, Methylene blue adsorption via maize silk powder: kinetic, equilibrium, thermodynamic studies and residual error analysis, Process Saf. Environ. Prot., 106 (2017) 191–202.
[45] F. Silva, L. Nascimento, M. Brito, K.D. Silva, W. Paschoal, R. Fujiyama, Biosorption of methylene blue dye using natural biosorbents made from weeds, Materials, 12 (2019) 2486.
[46] O. Hamdaoui, Adsorption of Cu(II) from aqueous phase by Cedar bark, J. Dispersion Sci. Technol., 38 (2017) 1087–1091.
[47] C. Djelloul, A. Hasseine, O. Hamdaoui, Adsorption of cationic dye from aqueous solution by milk thistle seeds: isotherm, kinetic and thermodynamic studies, Desal. Water Treat., 78 (2017) 313–320.
[48] M. Dogan, H. Abak, M. Alkan, Adsorption of methylene blue onto hazelnut shell: kinetics, mechanism and activation parameters, J. Hazard. Mater., 164 (2009) 172–181.
[49] P. Janos, H. Buchtova, M. Ryznarova, Sorption of dyes from aqueous solutions onto fly ash, Water Res., 37 (2003) 4938–4944.
[50] C. Djelloul, O. Hamdaoui, Removal of cationic dye from aqueous solution using melon peel as non-conventional low-cost sorbent, Desal. Water Treat., 52 (2014) 7701–7710.
[51] A. Hamzezadeh, Y. Rashtbari, S. Afshin, M. Morovati, M. Vosoughi, Application of low-cost material for adsorption of dye from aqueous solution, Int. J. Environ. Anal. Chem., doi:10.1080/03067319.2020.1720011.
[52] S. Lagergren, Zur theorie der sogenannten adsorption geloster stoffe. Kung-liga Svenska Vetenskapsakademiens. Handlingar, Band, 24 (1898) 1–39.
[53] G. Blanachard, M. Maunaye, G. Martin, Removal of heavy metals from waters by means of natural zeolites, Water Res., 18 (1984) 1501–1507.
[54] Y.S. Ho, G. McKay, The kinetics of sorption of basic dyes from aqueous solution by sphagnum moss peat, Can. J. Chem. Eng., 76 (1998) 822–827.

[55] K.G. Bhattacharyya, A. Sharma, Kinetics and thermodynamics of methylene blue sorption on neem (azadirachta indica) leaf powder, Dyes Pigm., 65 (2005) 51–59.
[56] I. Langmuir, The adsorption of gases on plane surfaces of glass, mica and platinum, J. Am. Chem. Soc., 40 (1918) 1361–1403.
[57] H.M.F. Freundlich, Über die adsorption in lösungen, Z. Phys. Chem., 57 (1906) 385–470.
[58] M.J. Temkin, V. Pyzhev, Recent medications to Langmuir isotherms, Acta Physiochim. USSR, 12 (1940) 217–222.
[59] Z. Derakhshan, M.A. Baghapour, M. Ranjbar, M. Faramarzian, Adsorption of Methylene Blue dye from aqueous solutions by modified pumice stone: kinetics and equilibrium studies, Health Scope, 2 (2013) 136–144.
[60] S. Rangabhashiyam, S. Lata, P. Balasubramanian, Biosorption characteristics of methylene blue and malachite green from simulated wastewater onto Carica papaya wood biosorbent, Surf. Interfaces, 10 (2018) 197–215.
[61] A.P.C. Alfredo, G.C. Gonçalves, V.S. Lobo, S.F. Montanher, Adsorção de azul de metileno em casca de batata utilizando sistemas em batelada e coluna de leito fixo, Rev. Virtual Quim., 7 (2015) 1909–1920.
[62] F. Afshariani, A. Roosta, Experimental study and mathematical modeling of biosorption of methylene blue from aqueous solution in a packed bed of microalgae Scenedesmus, J. Cleaner Prod., 225 (2019) 133–142.
[63] K.R. Hall, L.C. Eagleton, A. Acrivos, Vermeulen T. Pore and solid diffusion kinetics in fixed-bed adsorption under constant pattern conditions, Ind. Eng. Chem. Fundam., 5 (1966) 212–223.